CHAPTER-2

STUDY OF LINEAR STABILITY DYNAMICS IN COMPLEX VISCOELASTIC ASTROFLUIDS

Abstract: *A semi-analytic study on the evolutionary excitation dynamics of gravitational instability in a self-gravitating viscoelastic non-thermal polytropic complex uni-component fluid is carried out on the astro-scales of space and time. We apply a generalized gravitating hydrodynamic model. It concurrently considers the effects of fluid buoyancy, thermal fluctuations, volumetric expansion, and so forth.*[†] *A normal mode (local) analysis yields a quadratic linear dispersion relation with a unique set of multi-parametric coefficients. The analytical reliability is checked by comparing with the existing reports on purely ideal inviscid nebular fluid and non-ideal viscoelastic fluids in isolation. The stabilizing (destabilizing) and accelerating (decelerating) factors of the instability are illustratively explored. The instability features are judged in the light of both impure non-ideal viscoelastic fluid and pure ideal inviscid nebular fluid scenarios of real importance.*

2.1 INTRODUCTION

The dynamical mechanism of star and other bounded structure formation in the interstellar medium (ISM) is triggered by the so-called gravitational (Jeans) instability of self-gravitating fluids [1]. The self-gravitating fluids exhibit a rich spectrum of waves, instabilities, and oscillations on the astro-scales of space and time. As a result, agglomeration of matters take place in the astroclouds of ISM building up the early phase of bounded structure to form. The dynamics of the astrofluids, in addition to the Jeans criterion, gets modified due to the presence of various realistic inevitable physical factors.

Many researchers have investigated such gravitational instabilities and involved dynamics in different fluidic configurations in the past. They explored diversified underlying stabilizing and destabilizing agencies having great impact in the initiation processes of astrophysical proto-structures. Chandrasekhar have studied the effects of *uniform rotation* and *uniform magnetic field* on the evolutionary dynamics of gravitational instability in an infinite homogenous medium [2]. They have found that the instability dynamics is independent of both the rotation and field. However, the presence of weakly

[†]Karmakar, P. K. and Kalita, D., Dynamics of gravitational instability excitation in viscoelastic polytropic fluids. *Astrophysics and Space Science*, 363: 239. 1-11, 2018.

interacting massive particles (WIMPs) in interstellar gas cloud reduced the Jeans length, and Jeans mass. The instability of a gravitationally coupled viscoelastic system of neutral fluid and dark matter fluid has been addressed both in the linear regime [3, 4] as well as non-linear regime [5]. It has been shown semi-analytically that the instability has been significantly affected by the conjoint action of both viscosity and relaxation effects in a simplified way. Furthermore, the threshold for the onset of the instability occurs at lower wavenumbers in a viscoelastic medium against the conventional pure inviscid nebular fluid picture [6]. It can be clearly seen that the gravitational instability in such correlated viscoelastic media in the presence of all the possible realistic agencies has still been remaining as an unaddressed, unsolved and unexplored problem for years.

A comprehensive rigorous study of the non-local gravitational instability needs a proper inclusion of all the important fluid properties, such as polytropicity, buoyancy, thermal fluctuation, volumetric expansion, etc. This motivates us to report a new generalized viscoelastic fluid model to investigate the gravitational instability in the presence of all the above key realistic factors. A realistic instability analysis, as being presented herein, plays an important role in the structure formation mechanism in diversified realistic compact astro-cosmic structures and environs [2, 7]. It indeed forms the originality and basis of the current problem of the stability analysis. Thus, after implementing all the fluid complication in our model, the new basic set of the generalized fluid equations are carefully constructed, interpreted and analyzed.

2.2 PHYSICAL MODEL AND FORMALISM

A polytropic self-gravitating viscoelastic fluid model is considered in the fabric of a self-gravitational generalized uni-component hydrodynamic model configuration on the astrophysical scales of space and time. It simultaneously considers realistic factors, such as the effect of fluid buoyancy, thermal fluctuation, volumetric expansion, and so forth. The lowest-order viscoelasticity here comes from the collective correlative transport processes among the fluid constituent particles [3-6, 8-10]. The fluid is characterized with two kinds of viscosity, namely shear viscosity (offering resistance to flow), and the bulk viscosity (offering resistance to volumetric expansion). The main motivation behind considering the viscoelasticity is that viscoelastic fluids are rich in collective wave excitation processes under the combined action of both viscosity (energy dissipation source accounting for damping effects) and the elasticity (energy restoration source accounting for memory effects). In this context, it is worth mentioning that the nuclear matter in most of the

superdense compact objects and their surroundings is indeed viscoelastic (rheological) fluid in nature [6, 11]. In addition, this is a well-established generalized fact that cosmic fluids are highly viscoelastic in nature thereby exhibiting rich plethora of collective excitation of waves, oscillation and fluctuation [3-5, 7]. It is to be noted here that the role of plasma effects in such wave activities is ignored on the grounds that astro-cosmic fluids on a large scale are neutral in nature because of the negligible value of the ratio of the plasma Debye length to the instability scale length termed as the Jeans length [12].

It is a well-known fact that astrophysical macroscopic fluids are inhomogeneous and non-uniform in nature. A good number of transport activities keep on going even in the so-called equilibrium. It has been found that the presence of diversified diffusion-induced effects (such as, mass and thermal energy diffusion) noticeably modify the excitation of gravitational instability behaviours [13-15]. This motivates us to see whether we can find any possible diffusion-induced influence on the instability in complex our fluid model governed by a coupled set of generalized hydrodynamic (GH) equations.

The one-dimensional (1-D) evolutionary fluid dynamics is described by the continuity equation for the net flux-density conservation and momentum equation for the net force-density conservation in the customary notations [6, 9], respectively given as

$$\frac{\partial \rho}{\partial t}+\frac{\partial}{\partial x}(\rho v)=0\ , \tag{2.1}$$

$$\left[1+\tau_m\left(\frac{\partial}{\partial t}+v\frac{\partial}{\partial x}\right)\right]\left[\rho\left(\frac{\partial}{\partial t}+v\frac{\partial}{\partial x}\right)v+\rho(1+\gamma T)\frac{\partial \psi}{\partial x}+\frac{c_s^2}{\Gamma}\frac{\partial \rho}{\partial x}\right]=\left[\varsigma+\frac{4}{3}\eta\right]\frac{\partial^2 v}{\partial x^2}\,, \tag{2.2}$$

where, ρ, v, τ_m, γ, T, Γ, ψ, ς and η are the fluid density, flow velocity, viscoelastic relaxation time, volumetric expansion coefficient, fluid temperature, polytropic exponent, gravitational potential, shear viscosity coefficient, and bulk viscosity coefficient, respectively. The symbol, $c_s=\left[\Gamma k_B T_0/m\right]^{1/2}$, denotes the normal sound phase speed with *m* as the constituent mass of the fluid and $k_B=1.38\times10^{-23}$ J K^{-1} as the Boltzmann constant. The macroscopic (bulk incompressible fluid) state is described by the evolution equations relating the fluid pressure (*P*), and fluid density (ρ), given as

$$\left(\frac{\partial}{\partial t}+v\frac{\partial}{\partial x}\right)\left(P\rho^{-\Gamma}\right)=0\,, \tag{2.3}$$

The thermal diffusion and mass diffusion processes are given as

$$\frac{\partial T}{\partial t}+v\frac{\partial T}{\partial x}=K_T\frac{\partial^2 T}{\partial x^2}\,, \tag{2.4}$$

$$\frac{\partial \rho}{\partial t} + v \frac{\partial \rho}{\partial x} = K_M \frac{\partial^2 \rho}{\partial x^2} \ , \tag{2.5}$$

where, K_T and K_M are the thermal diffusivity and mass diffusivity, respectively.

The considered fluid is finally closed by the Poisson equation relating the spatial distribution of the non-local gravitational potential (ψ) with the source fluid density as

$$\frac{\partial^2 \psi}{\partial x^2} = 4\pi G(\rho - \rho_0), \tag{2.6}$$

where, $G = 6.67 \times 10^{-11}$ N m^2 kg^{-2} is the universal (Newtonian) gravitational constant signifying the coupling strength of gravitational interaction of matter and ρ_0 is the hydrostatic equilibrium density accounting for the so-called Jeans swindle [1, 16, 17]. The swindle considered here is an ad-hoc homogenization assumption needed for ignoring the zeroth-order force field effects on the grounds that the inward self-gravitational attraction in the fluid is balanced by the outward expansive repulsion in the fluid caused by the cosmic pressure force effects in the initially homogeneous equilibrium fluid configurations [1, 16, 17]. It judiciously allows us to perform a local normal mode analysis around the initially hydrostatic homogeneous equilibrium of the macroscopic bulk fluidic state.

A standard normalization technique [3-5] is used to execute a scale-free non-dimensional analysis. The normalized set of equations (2.1)-(2.6), thus constructed, are respectively given as

$$\frac{\partial \rho^*}{\partial \tau} + \frac{\partial}{\partial \xi}\left(\rho^* M\right) = 0, \tag{2.7}$$

$$\left[1 + \frac{\tau_m}{\tau_J}\left(\frac{\partial}{\partial \tau} + M \frac{\partial}{\partial \xi}\right)\right]\left[c_s \rho_0 \rho^* \left(\frac{\partial}{\partial \tau} + M \frac{\partial}{\partial \xi}\right) M + c_s \rho_0 \rho^* \left(1 + \gamma T_0 T^*\right) \frac{\partial \Psi}{\partial \xi} + \frac{c_s \rho_0}{\Gamma} \frac{\partial \rho^*}{\partial \xi}\right]$$

$$= \frac{1}{\lambda_J}\left(\varsigma + \frac{4}{3}\eta\right) \frac{\partial^2 M}{\partial \xi^2}, \tag{2.8}$$

$$\left(\frac{\partial}{\partial \tau} + M \frac{\partial}{\partial \xi}\right)(P^* \rho^{*-\Gamma}) = 0, \tag{2.9}$$

$$\frac{\partial T^*}{\partial \tau} + M \frac{\partial T^*}{\partial \xi} = \left(\frac{K_T}{c_s \lambda_J}\right) \frac{\partial^2 T^*}{\partial \xi^2}, \tag{2.10}$$

$$\frac{\partial \rho^*}{\partial \tau} + M \frac{\partial \rho^*}{\partial \xi} = \left(\frac{K_M}{c_s \lambda_J}\right) \frac{\partial^2 \rho^*}{\partial \xi^2}, \tag{2.11}$$

$$\frac{\partial^2 \Psi}{\partial \xi^2} = \rho^* - 1. \tag{2.12}$$

Here, $\xi = x/\lambda_J$ and $\tau = t/\tau_J$ are the normalized forms of distance and time, where $\lambda_J = c_s/\tau_J$ is the Jeans scale length and $\tau_J = \omega_J^{-1} = \left(4\pi\rho_0 G\right)^{-1/2}$ is the Jeans time scale, respectively. Furthermore, $\Psi = \psi/c_s^2$, $\rho^* = \rho/\rho_0$, $P^* = P/P_0$, and $T^* = T/T_0$ denote the normalized gravitational potential, fluid density, pressure and temperature, respectively. Here, P_0 and T_0 are the equilibrium values of the pressure and temperature, respectively. Also, $M = v/c_s$ is the Mach number (normalized flow speed) of the bulk viscoelastic fluid. Needless to say, '1' in equation (2.12), as previously in equation (2.6), accounts for the so-called Jeans swindle [1, 16, 17].

We now allow the fluid model relevant parameters (*F*) to undergo small-scale linear perturbations (F_1) around their local hydrostatic homogenous equilibrium parametric values (F_0) on the grounds that the perturbations evolve as sinusoidal homology signals [5] given as

$$F(\xi,\tau) = F_0 + F_1 \exp\left[-i(\Omega\tau - K\xi)\right], \tag{2.13}$$

$$F = [\,\rho^* \quad M \quad T^* \quad P^* \quad \Psi\,]^{\mathrm{T}}, \tag{2.14}$$

$$F_0 = [1 \quad 0 \quad 1 \quad 1 \quad 0]^{\mathrm{T}}, \tag{2.15}$$

$$F_1 = [\,\rho_1^* \quad M_1 \quad T_1^* \quad P_1^* \quad \Psi_1\,]^{\mathrm{T}}. \tag{2.16}$$

In the newly defined wave-space (Ω, K), the linear operators transform as $\partial/\partial\xi \to (+iK)$ and $\partial/\partial\tau \to (-i\Omega)$; where Ω is the Jeans-normalized angular frequency and K is the Jeans-normalized angular wavenumber. Accordingly, equations (2.7)-(2.12) get respectively auto-transformed as

$$M_1 = \frac{\Omega\rho_1^*}{K}, \tag{2.17}$$

$$\left[1 - i\Omega\frac{\tau_m}{\tau_J}\right]\left[-\Omega c_s\rho_0 M_1 + Kc_s\rho_0(1+\gamma T_0)\Psi_1 + \frac{Kc_s\rho_0}{\Gamma}\rho_1^*\right] = iK^2\left(\frac{M_1}{\lambda_J}\right)\left(\varsigma + \frac{4}{3}\eta\right), \tag{2.18}$$

$$P_1^* = \Gamma\rho_1^*, \tag{2.19}$$

$$i\Omega = -\frac{K_T}{c_s\lambda_J}K^2, \tag{2.20}$$

$$i\Omega = -\frac{K_M}{c_s\lambda_J}K^2, \tag{2.21}$$

$$\Psi_1 = -\frac{\rho_1^*}{K^2}. \tag{2.22}$$

Substitution of the expression for M_1 from equation (2.17) and Ψ_1 from equation (2.22) in equation (2.18) yields

$$\left[1 - i\Omega\frac{\tau_m}{\tau_J}\right]\left[-\frac{\Omega^2 c_s\rho_0}{K} - \frac{c_s\rho_0(1+\gamma T_0)}{K} + \frac{Kc_s\rho_0}{\Gamma}\right] = \frac{iK\Omega}{\lambda_J}\left(\varsigma + \frac{4}{3}\eta\right). \tag{2.23}$$

Thus, the various dispersive properties of the gravitational instability under consideration is dictated by the generalized dispersion relation, equation (2.23), in full form under the active influence of all the adopted hydrodynamic realistic properties. Comparing the imaginary parts on both sides of equation (2.23), one obtains the reduced form of the modified dispersion relation involving all the considered key fluid effects as

$$\Omega = \left[\frac{K^2}{\Gamma}\left(1 + \frac{\chi}{n_0\tau_m k_B T_0}\right) - (1+\gamma T_0)\right]^{\frac{1}{2}}, \tag{2.24}$$

where, $n_0 = \rho_0/m$ is the equilibrium number density of the fluid constituents, $n = 1/(\Gamma - 1)$ is the polytropic index [2], and $\chi = [\varsigma + (4/3)\eta]$ is the effective generalized viscosity of the fluid. Similarly, another reduced form of the dispersion relation could be obtained by comparing the real parts of equation (2.23), but excluded here due to over-simplicity in it.

Let us now have further reliability checkups on equation (2.24) by reductive comparative analysis in the light of the previous results [1, 6]. If $\gamma = 0$ and $\Gamma = 1$, then equation (2.24) reduces to

$$\Omega = \left[K^2\left(1 + \frac{\chi}{n_0\tau_m k_B T_0}\right) - 1\right]^{\frac{1}{2}}, \tag{2.25}$$

which is the normalized form of the dispersion relation for the gravitational instability in a viscoelastic fluid as reported previously [6]. Moreover, if viscoelastic effects are ignored, for which $\chi = 0$, then equation (2.24) simply gets transformed into

$$\Omega = \left[K^2 - 1\right]^{\frac{1}{2}}, \tag{2.26}$$

which is the well-familiar normalized form of the usual gravitational dispersion relation in pure inviscid nebular fluids as previously reported by Jeans [1]. A close comparison between equations (2.25)-(2.26) clearly indicates how the usual Jeans instability gets modified due to inclusion of viscoelasticity in our proposed model. Evidently, the analytical

results on the proposed dispersion relation (equation (2.24)) have a two-fold reliability validation via equations (2.25)-(2.26).

It is clearly noticeable from equation (2.24) that the perturbations undergo dynamic growth provided the condition $\left[\left(K^2/\Gamma\right)\left(1+\left(\chi/n_0\tau_m k_B T_0\right)\right)\right] < \left(1+\gamma T_0\right)$ is well-fulfilled. In that case, equation (2.24) reveals the growth rate $\left(\Omega_i\right)$ of the fluctuations given as

$$\Omega_i = \left[\left(1+\gamma T_0\right) - \frac{K^2}{\Gamma}\left(1+\frac{\chi}{n_0\tau_m k_B T_0}\right)\right]^{\frac{1}{2}}. \tag{2.27}$$

It is interesting to note from equation (2.27) that the growth rate of the instability is affected by the conjoint action of polytropicity, buoyancy, thermal fluctuations, volumetric expansion and viscoelasticity. If we assume that $K \approx 0$, then equation (2.27) gives

$$\Omega_i = \left(1+\gamma T_o\right)^{1/2}. \tag{2.28}$$

It is seen from equation (2.28) that the growth rate depends only on the volumetric expansion $\left(\gamma T_0\right)$ in this limiting case ($K \approx 0$). In this case, the growth rate $\left(\Omega_i\right)$ attains the maximum value (>1) as given by equation (2.28). Thus, the volumetric expansion acts as a destabilizing agency to the fluctuations. On the other hand, when $K \neq 0$, the effect of other parameters comes into play to reduce the instability growth rate. It happens due to the negative contribution towards the instability (equation (2.27)). Thus, it is clearly evident that the volume expansion acts as a growth-enhancer and the combined action of all other factors acts as a growth-reducer.

Now, the phase velocity and the group velocity of the fluctuations derived from equation (2.24) can respectively be derived and written as

$$V_p = \frac{\Omega}{K} = \left[\frac{1}{\Gamma}\left(1+\frac{\chi}{n_0\tau_m k_B T_0}\right) - \frac{\left(1+\gamma T_0\right)}{K^2}\right]^{\frac{1}{2}}, \tag{2.29}$$

$$V_g = \frac{d\Omega}{dK} = \left[\frac{1}{\Gamma}\left(1+\frac{\chi}{n_0\tau_m k_B T_0}\right)\right]\left[\frac{1}{\Gamma}\left(1+\frac{\chi}{n_0\tau_m k_B T_0}\right) - \frac{\left(1+\gamma T_0\right)}{K^2}\right]^{-\frac{1}{2}}. \tag{2.30}$$

The multiplicative inter-relation between V_p and V_g of the fluctuations can be derived as

$$V_p\, V_g = \frac{1}{\Gamma}\left(1+\frac{\chi}{n_0\tau_m k_B T_o}\right). \tag{2.31}$$

For an accuracy checkup of equation (2.31), let us consider an ideal isothermal inviscid situation of the complex fluid. In that case, we have $\chi = 0$ and $\Gamma = 1$. As a result, equation (2.31) reduces to

$$V_p \, V_g = 1, \tag{2.32}$$

which in the unnormalized (dimensional) form can be transformed into

$$v_p \, v_g = c_s^2 . \tag{2.33}$$

Thus, a well-established multiplicative inter-relationship between the phase velocity (v_p) and the group velocity (v_g) for the gravitational instability via the acoustic phase speed (c_s) in the unnormalized form is revealed in equation (2.33). Applying a similar procedure, the divisional inter-relationship between v_p and v_g can be derived as

$$\frac{v_p}{v_g} = 1 - (1 + \gamma T_0)\left[\frac{K^2}{\Gamma}\left(1 + \frac{\chi}{n_0 \, \tau_m \, k_B \, T_0}\right)\right]^{-1} . \tag{2.34}$$

It is clearly evident from equation (2.34) that the strength of phase transport is weaker than that of group kinematic counterpart ($v_p < v_g$). The main implication herein is that the collective viscoelastic wave transport features in the proposed stability work are faster than those associated with other wave activities available in the literature. The present investigation is focally intended to explore the microphysical insights of the growth (equation (2.27)) and the propagatory features (equations (2.29)-(2.30)) associated with the gravitational instability. We execute a numerical illustrative analysis to depict the dynamical features as shown in the next section.

2.3 RESULTS AND DISCUSSIONS

An evolutionary theoretical model is constructed to investigate the gravitational instability dynamics supported in a complex viscoelastic fluid on the astrophysical scales of space and time. A generalized linear dispersion relation (quadratic in degree) is obtained by a standard method of linear local normal mode analysis. The local dispersion relation (equation (2.24)) is numerically analysed to unveil the microphysical features of the instability illustratively. The different judicious input values for the numerical analysis are adopted from different reliable sources centred around the dwarf-family available in the literature [2, 18-20]. The investigated results obtained here are graphically depicted and illustrated in figures 2.1-2.6.

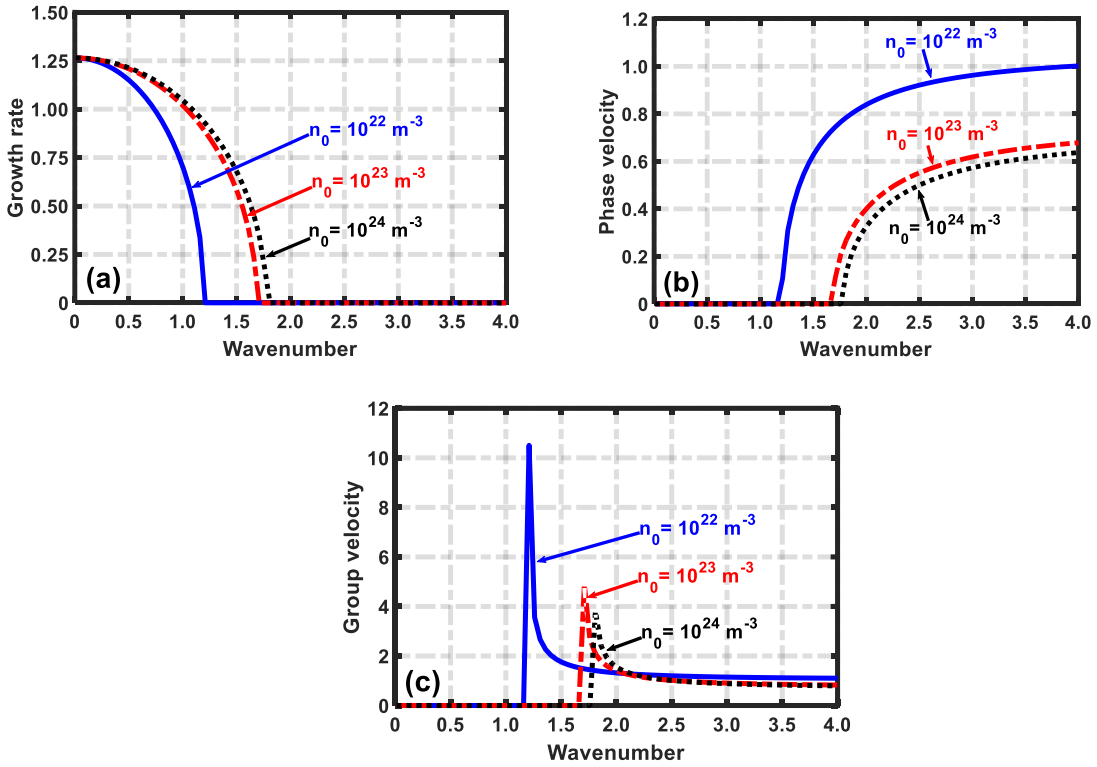

Figure 2.1: *Profile of the Jeans-normalized (a) growth rate* (Ω_i)*, (b) phase velocity* (V_p)*, and (c) group velocity* (V_g) *with variation in the Jeans-normalized wavenumber* (K) *for different equilibrium number density* (n_0) *values.*

In figure 2.1, we show the profile of the Jeans-normalized (a) growth rate (Ω_i), (b) phase velocity (V_p), and (c) group velocity (V_g) for different values of the equilibrium fluid particle concentration (n_0) with variation in the Jeans-normalized wavenumber (K). The distinct lines correspond to different concentrations as $n_0 = 10^{22}$ m^{-3} (blue solid line), $n_0 = 10^{23}$ m^{-3} (red dashed line), and $n_0 = 10^{24}$ m^{-3} (black dotted line), respectively [20, 21]. The different input values used are the mean temperature $T_0 = 60$ K [19], polytropic index $n = 1$ [2], volumetric expansion coefficient $\gamma = 10^{-2}$ K^{-1} [18], effective generalized viscosity $\chi = 10^{-1}$ kg m^{-1} s^{-1} [20], and viscoelastic relaxation time $\tau_m = 10^{-2}$ s . It is seen that, for a given n_0, the growth rate of the fluctuations decreases towards the high-*K* regime relative to the Jeansian critical value (figure 2.1(a)). In other words, only the long-wavelength (gravitational) fluctuations undergo active growth leaving the short-

wavelength (acoustic) components marginally stabilized. In addition, as the n_0- value increases, the growth rate shifts towards the high-*K* regime (figure 2.1(a)). It indicates that denser the fluid, higher the growth of the mechanical perturbations in the fluid, and vice-versa. Moreover, the magnitude of both the phase velocity (figure 2.1(b)) and group velocity (figure 2.1(c)) of the fluctuation reduces with the n_0-increment, and vice-versa. Thus, it can be inferred that n_0 acts as a deceleration agent to the instability dynamics.

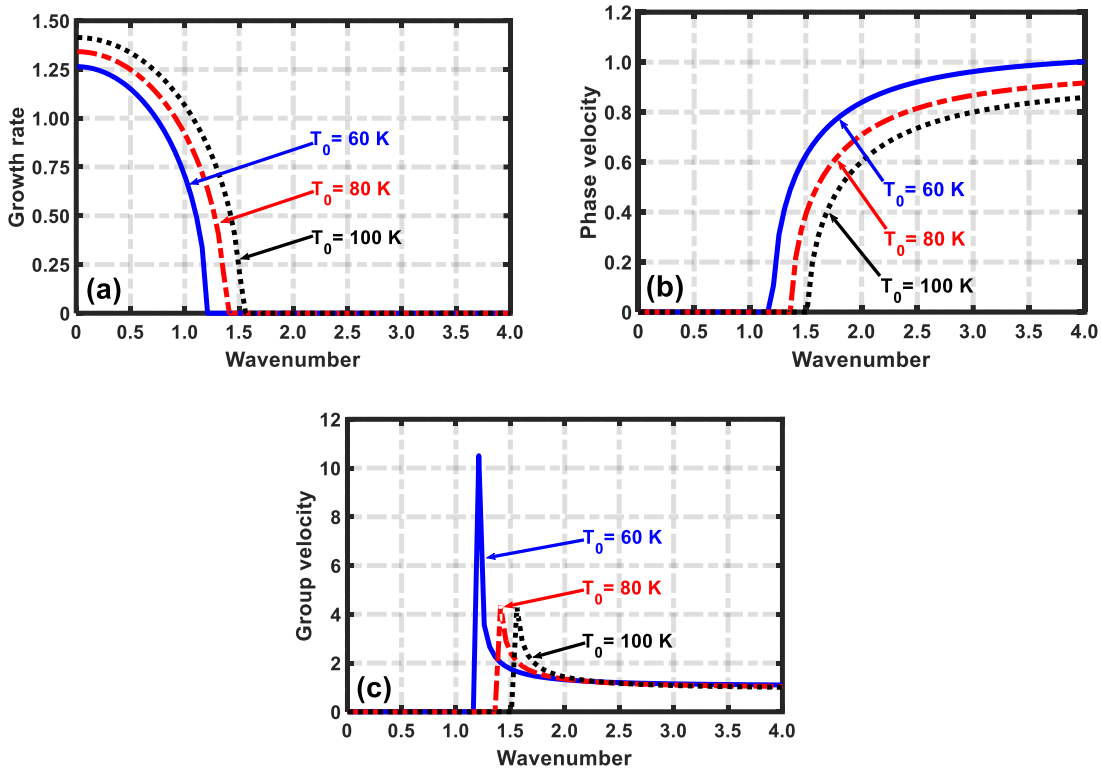

Figure 2.2: *Same as figure 2.1, but with a fixed* $n_0 = 10^{22}$ m^{-3} *for different* T_0 – *values.*

As in figure 2.2, we portray the same as figure 2.1, but with a fixed $n_0 = 10^{22}$ m^{-3} for different values of the equilibrium fluid temperature (T_0). It is seen that, for a given T_0 , the growth decreases towards the high-*K* regime (figure 2.2(a)). As T_0 increases, the growth rate increases, and vice-versa. It indicates that hotter fluids are more unstable, and vice-versa. The phase velocity (figure 2.2(b)) and group velocity (figure 2.2(c)) evolve in the same fashion as discussed previously (figure 2.1). Thus, T_0 acts as destabilizing and decelerating agency to the fluid instability evolution under the action of self-gravity.

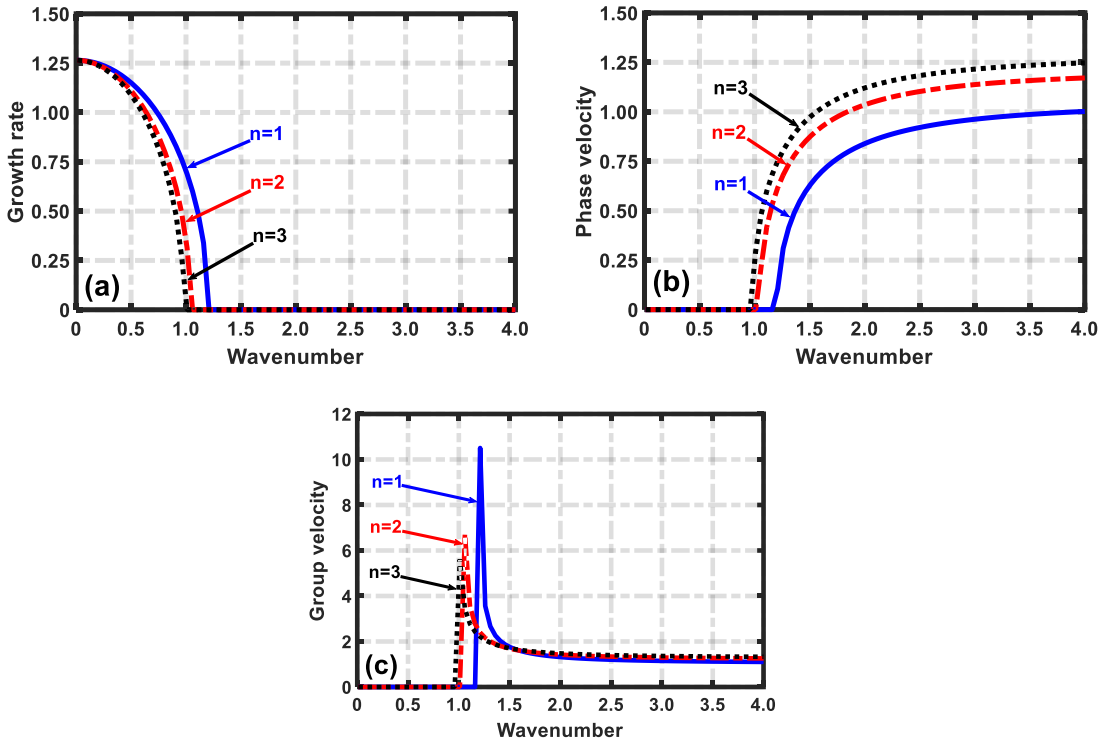

Figure 2.3: *Same as figure 2.1, but with a fixed* $n_0 = 10^{22}$ m^{-3} *for different* $n-$ *values.*

As in figure 2.3, we display the same as figure 2.1, but with a fixed equilibrium density $n_0 = 10^{22}$ m^{-3} for different values of polytropic index (n). It is seen that, for a given *n*, the growth rate decreases towards the high-*K* regime (figure 2.3(a)). It hereby indicates that only the long-wavelength (gravitational) fluctuations undergo active growth. Furthermore, as the $n-$value increases, the growth rate shifts towards the low-*K* (long-wavelength) regime (figure 2.3(a)). It implicates that, bigger the *n*-value, more stable is the fluid. Moreover, the magnitude of the phase velocity (figure 2.3(b)) increases and that of the group velocity (figure 2.3(c), wave packet) decreases towards the low-*K* regime. This correlation between the phase velocity and group velocity is supported by our obtained two-fold velocity relationship (equation (2.31)). Thus, it may be inferred that *n* acts as both stabilizing and decelerating agents towards the dynamical fluctuations.

Like-wise, in figure 2.4, we depict the same as figure 2.1, but with a fixed $n_0 = 10^{22}$ m^{-3} for different values of effective generalized viscosity (χ). It is found that the growth rate (figure 2.4(a)) of the instability varies in a similar pattern as in (figure 2.3(a)) for a given polytropic index, *n*. As the $\chi-$value increases, the magnitude of both the phase

velocity (figure 2.4(b)), and the group velocity (figure 2.4(c)) increases, and vice-versa. Thus, χ acts as both stabilizing and accelerating agents for the instability.

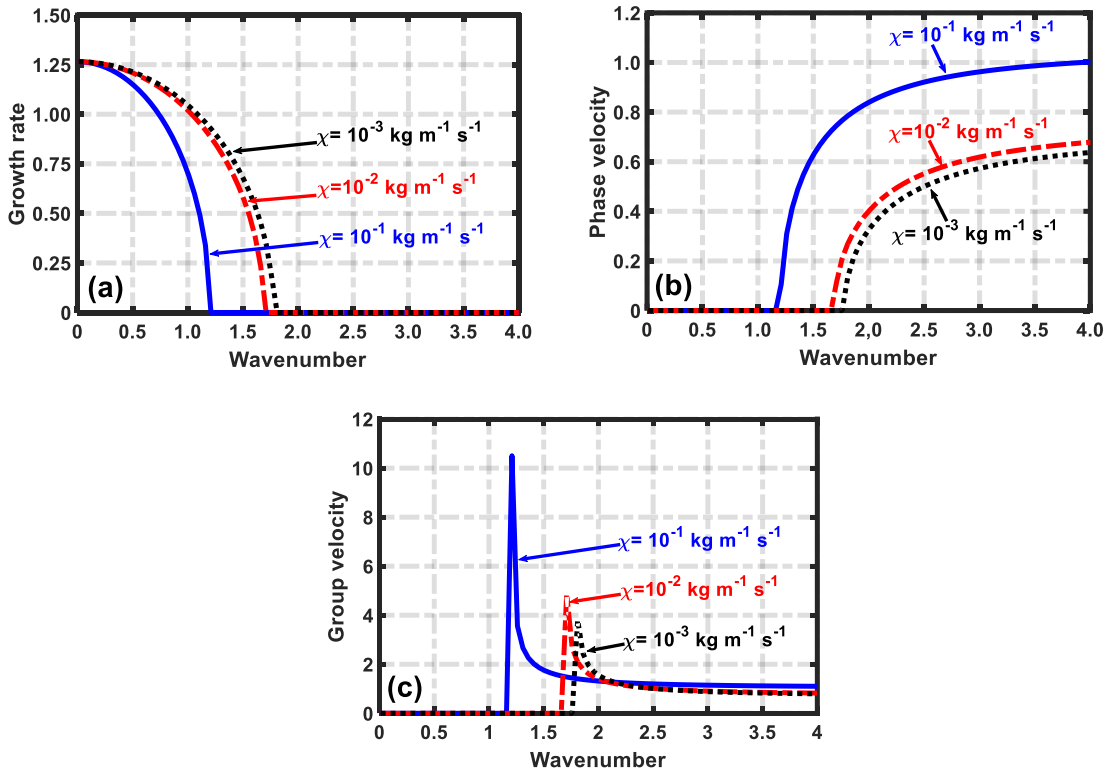

Figure 2.4: *Same as figure 2.1, but with a fixed* $n_0 = 10^{22}$ m^{-3} *for different* $\chi-$ *values.*

Parallelly, as in figure 2.5, we show the same as figure 2.1, but with a fixed $n_0 = 10^{22}$ m^{-3} for different values of viscoelastic relaxation time (τ_m). The growth rate (figure 2.5(a)), phase velocity (figure 2.5(b)), and group velocity (figure 2.5(c)) vary in a similar fashion as in the case of the n_0-variation highlighted above (figure 2.1). Thus, τ_m plays as both stabilizing and decelerating influential agents to the instability.

Lastly, as in figure 2.6, we present comparative profiles of the normalized (a) growth rate (Ω_i), (b) phase velocity (V_p), and (c) group velocity (V_g) with variation in the Jeans-normalized wavenumber (K) for different fluid configurations. The different lines link to (i) pure inviscid nebular fluid model (blue solid line) [1], (ii) viscoelastic fluid model (red dashed line) [6], and (iii) our complex viscoelastic fluid (black dotted line), respectively. In pure inviscid nebular fluid model (case (i)), we take the mean temperature $T_0 = 60$ K, equilibrium number density $n_0 = 10^{22}$ m^{-3}, and polytropic exponent

$\Gamma = \left(1 + n^{-1}\right) = 1$. In viscoelastic fluid model (case (ii)), we take the effective generalized viscosity $\chi = 10^{-1}$ kg m^{-1} s^{-1}, and viscoelastic relaxation time $\tau_m = 10^{-2}$ s in addition to case (i). In our complex fluid model (case (iii)), we take the polytropic index $n = 1$, volumetric expansion coefficient $\gamma = 10^{-2}$ K^{-1} in addition to case (ii). The pure Jeans growth extends over a critical Jeans length scale alone (K=1). The viscoelastic Jeans growth spectrally extends over a sub-critical Jeans length (K<1). The complex Jeans growth extends over a super-critical Jeans length (K>1). At the same time, both the pure Jeans and viscoelastic Jeans growths achieve a common maximum value of unity in the same K-regime; whereas, the complex Jeans growth surpasses the former two (in both Ω_i, K). As a consequence, all the realistic factors considered in our complex model afresh combine together hand-in-hand to both enhance (in Ω_i) and broaden (in K) the Jeans instability against the pure idealistic simpler situations mentioned previously. In other words, it is seen that viscoelastic fluids are the most stable, our complex fluid is the most unstable and pure ideal nebular fluid is lying in between the two. The reason behind this is that all the factors considered before lead the fluid system towards reduced stability. It is only the combined effects of the volume expansion and polytropicity (which are not considered before) lead the complex fluid of our interest towards enhanced instability.

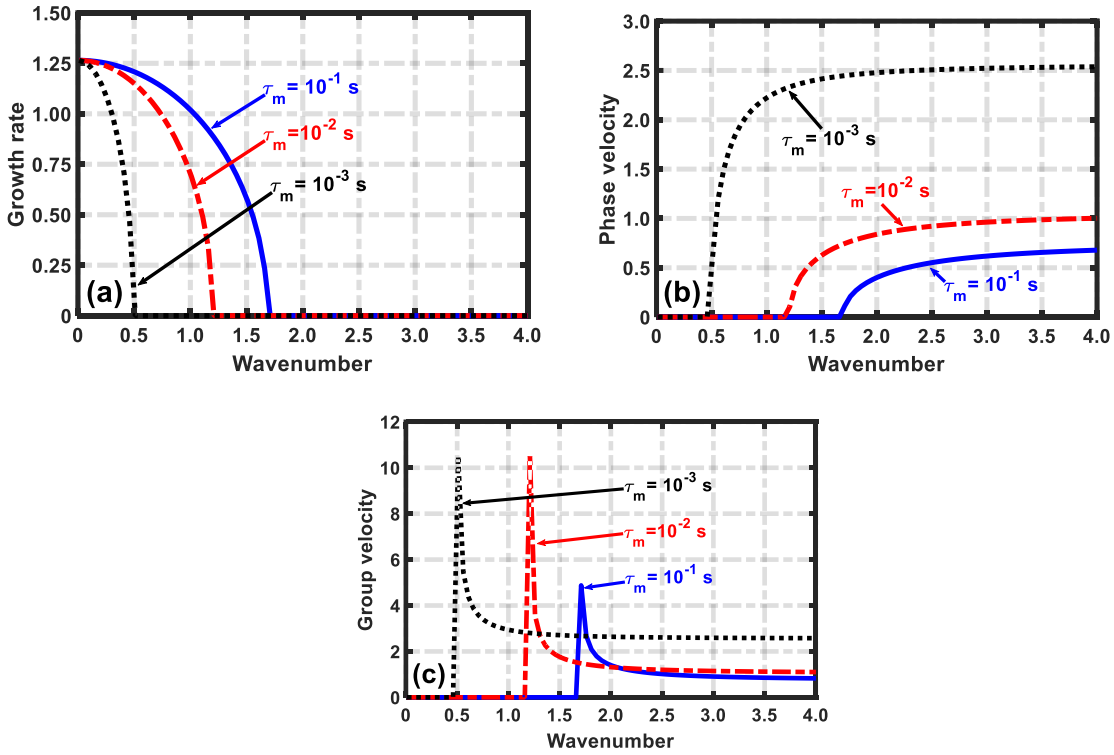

Figure 2.5: *Same as figure 2.1, but with a fixed* $n_0 = 10^{22}$ m^{-3} *for different* $\tau_m -$ *values.*

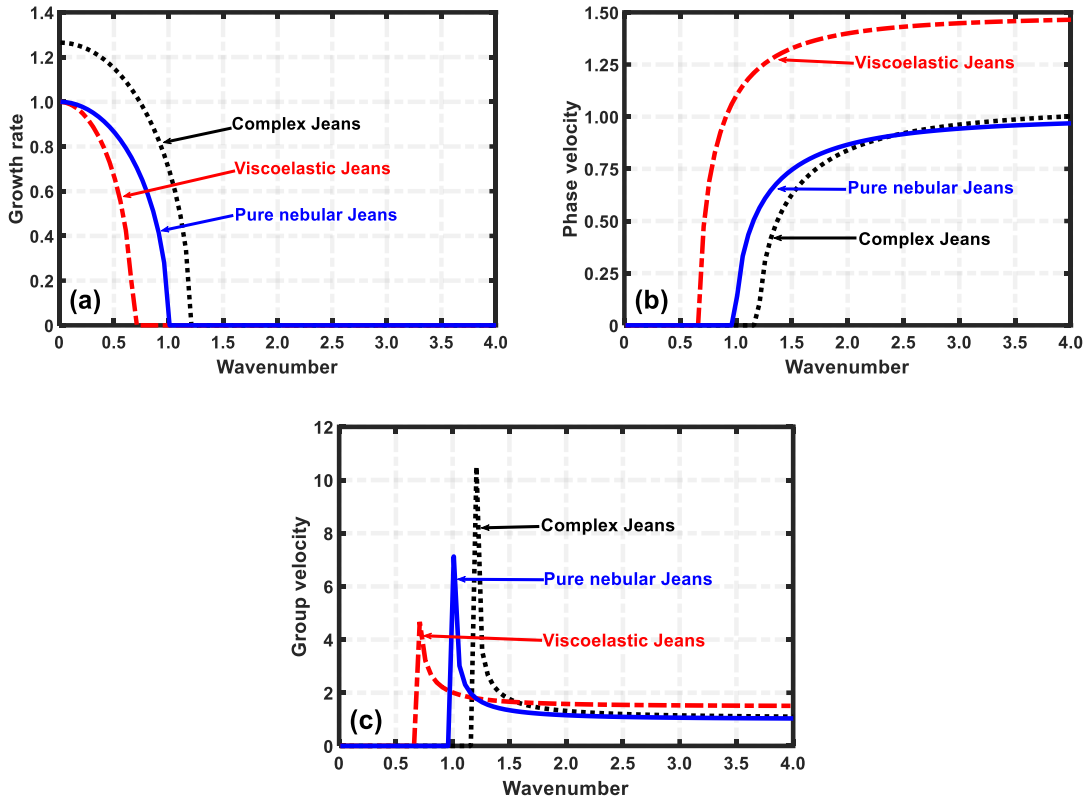

Figure 2.6: *Same as figure 2.1, but for different fluid configurations.*

In summary, it may, consequently, be conjectured in a nutshell that the various stabilizing (destabilizing) and accelerating (decelerating) sources stemming from the considered complex fluid properties affecting the dynamics of the instability are numerically identified and characterized. Besides, a comparative numerical standpoint is provided to judge the significance features of our instability analysis over the previously reported results by others [1, 6]. In the all the cases discussed above (figures 2.1-2.6), the gravitational instability growth achieved the maximum value $\left(\Omega_i \geq 1\right)$ in the localized large-scale gravitational wavelength regime $\left(K \geq 1\right)$; elsewhere, the growth decreases to a non-negative zero-value. It indicates that the simultaneously coupled action of growth and decay in the considered fluid model is not supported, which may in principle, be possible for an electrified self-gravitating fluid under the combined action of various long-range forces. As a reliability checkup of the investigated examination, the key model findings more specifically proposed here go in good accord with all the earlier predictions and results made by others separately in the context of gravitating fluid instability dynamics [1-6, 22].

2.4 CONCLUSIONS

We investigate herein the long-range self-gravitational instability dynamics in a large scale viscoelastic fluid medium. The formalism is centred in a self-gravitational GH model configuration of realistic astronomical relevancy. The key influential properties are simultaneously considered in the dynamical configurations. In the fabric of one component hydrodynamic fluid, it considers fluid polytropicity, non-thermality, buoyancy effects, and so on. A new set of base evolution equations is systematically built up in the fabric of the considered factors. The fluid configuration is assumed initially to be in a hydrostatic homogenous equilibrium. A local linear normal analysis decouples the perturbed fluid equations into a linear generalized dispersion relation of quadratic nature having a unique set of multi-parametric coefficients. It is worthwhile to mention here that the free energy source for such unipolar instabilities arises from the fluid currents driven by the self-gravity itself. More simply, the free energy source here is associated with the non-local fluid self-gravity. The investigated instability remains unaffected due to the considered thermo-mechanical diffusion processes unlike the traditional instability mechanisms in the presence of gravitational effects. The reliability of our analytic calculation scheme is fruitfully bolstered in light of the exact reproducibility of the well-established dispersion relations for the similar gravitational instability in both purely non-ideal viscoelastic fluid and purely ideal inviscid nebular fluid in isolation available widely in the literature [1, 6].

A numerical illustrative platform is subsequently put forward to explore the propagatory features of the gravitational instability in the light of judicious input multi-parametric values available in the literature. An inter-relationship between the phase velocity and group velocity is reliably established in a perfect match with the existing usual one. The stabilizing (destabilizing) and accelerating (decelerating) factors affecting the instability evolution are explored. It is shown that the equilibrium fluid concentration, polytropic index, effective generalized viscosity and viscoelastic relaxation time act as stabilizing factors to the fluid against the self-gravitational collapse dynamics. In contrast, the equilibrium temperature behaves as a destabilizing agency. In addition, it is only the effective generalized viscosity that boosts up the instability (as a wave-packet). It is further speculated that the equilibrium concentration, equilibrium temperature and viscoelastic relaxation time accounting for the memory effects shift the instability growth towards the smaller wavelength regimes (high-K). On the contrary, the polytropic index and the effective generalized viscosity shift the instability growth towards the longer wavelength

domains (low-*K*). At the last, a comparative foundation is numerically illustrated to examine the validation of our proposed instability analysis reliably in the auspice of the Jeans instability naturalistically triggered in an ideal inviscid nebular fluid [1] and non-ideal viscoelastic fluid [6] as elaborately described in the literature.

The proposed model analysis can be widely continued to explore the non-linear eigen-mode structures existing in diversified realistic astronomical fluid environments with the help of applied perturbative techniques [23, 24]. In addition, the semi-analytic findings reported herein could be commodiously helpful in understanding the gravito-thermally triggered coupled collective instability and saturation phenomena in super-dense compact astrophysical objects and their circumvent ambient atmospheres. This is because of the well-established fact that this class of compact astro-structures indeed exhibit a plethora of conjoint correlative heterogeneous coupling effects in the form of wide-range collective viscoelastic wave excitations and evolutionary processes of real astronomical value [2, 7].

REFERENCES

[1] Jeans, J. H. The stability of a spherical nebula. *Philosophical Transactions of the Royal Society,* 199: 1-53, 1902.

[2] Chandrasekhar, S. *An Introduction to the Study of Stellar Structure*. University of Chicago Press, Chicago, 1938.

[3] Karmakar, P. K. and Das, P. Instability analysis of cosmic viscoelastic gyro-gravitating clouds in the presence of dark matter. *Astrophysics and Space Science,* 362: 142. 1-13, 2017.

[4] Karmakar, P. K. and Das, P. Stability of gravito-coupled complex gyratory astrofluids. *Astrophysics and Space Science,* 362: 115. 1-9, 2017.

[5] Das, P. and Karmakar, P. K. Instability behaviour of cosmic gravito-coupled correlative complex bi-fluidic admixture. *Europhysics Letters,* 120: 19001. p1-p7, 2017.

[6] Janaki, M. S., Chakrabarti, N., and Banerjee, D. Jeans instability in a viscoelastic fluid. *Physics of Plasmas,* 18: 012901. 1-5, 2011.

[7] Brevik, I. Temperature variation in the dark cosmic fluid in the late universe. *Modern Physics Letters A,* 31: 1650050. 1-12, 2016.

[8] Frenkel, J. *Kinetic Theory of Liquids.* Oxford University Press, Oxford, 1946.

[9] Gresho, P. M. and Sani, R. L. *Incompressible Flow and the Finite Element Method.* Wiley, New York, 1998.

[10] Raymond, J. and Skarda, L. Convective Instability of a Gravity Modulated Fluid Layer With Surface Tension Variation. AIAA-98-2599, New Mexico, 1998.

[11] Bastrukov, S. I., Weber, F., and Podgainy, D. V. On the stability of global non-radial pulsations of neutron stars. *Journal of Physics G: Nuclear and Particle Physics*, 25: 107-127, 1999.

[12] Dwivedi, C. B., Karmakar, P. K., and Tripathy, S. C. A gravito-electrostatic sheath model for surface origin of subsonic solar wind plasma. *Astrophysical Journal*, 663: 1340-1353, 2007.

[13] Adham-Khodaparast, K., Kawaji, M., and Antar, B. N. The Rayleigh–Taylor and Kelvin–Helmholtz stability of a viscous liquid–vapor interface with heat and mass transfer. *Physics of Fluids*, 7: 359-364, 1995.

[14] Hujeirat, A. Ambipolar diffusion in star-forming clouds. *Astronomy and Astrophysics*, 334: 742-745, 1998.

[15] Hosseinirad, M., Naficy, K., Abbassi, S., and Roshan, M. Gravitational instability of filamentary molecular clouds, including ambipolar diffusion. *Monthly Notices of the Royal Astronomical Society*, 465: 1645-1653, 2017.

[16] Binney, J. and Tremaine, S. *Galactic Dynamics.* Princeton University Press, Princeton, 1987.

[17] Mo, H., Van den Bosch, F., and White, S. *Galaxy Formation and Evolution.* Cambridge University Press, Cambridge, 2010.

[18] Schwalbe, L. and Grilly, E. Thermal expansion of liquid normal hydrogen between 18.8 and 22.2 K. *Journal of Research of the National Bureau of Standards*, 89: 317-323, 1984.

[19] Tielens, A. G. G. M. *The Physics and Chemistry of the Interstellar Medium.* Cambridge University Press, Cambridge, 2005.

[20] Borah, B., Haloi, A., and Karmakar, P. K. A generalized hydrodynamic model for acoustic mode stability in viscoelastic plasma fluid. *Astrophysics and Space Science*, 361: 165. 1-11, 2016.

[21] Kalita, D. and Karmakar, P. K. Nonlinear dynamics of gravitational instability in complex viscoelastic astrofluids. *AIP Advances*, 8: 085207, 2018.

[22] Tsiklauri, D. Jeans instability of interstellar gas clouds in the background of weakly interacting massive particles. *Astrophysical Journal*, 507: 226-228, 1998.

[23] Karmakar, P. K. and Dutta, P. Nonlinear eigen-structures in star-forming gyratory nonthermal complex molecular clouds. *Physics of Plasmas*, 25: 012306. 1-9, 2018.

[24] Das, P. and Karmakar, P. K. Dynamics of flow-induced instability in gyrogravitating complex viscoelastic quantum fluids. *AIP Advances*, 8: 085209. 1-14, 2018.